# EFFECT OF TWIN TUNNEL GEOMETRY ON LINING PERFORMANCE AND GROUND SETTLEMENT: A CASE STUDY

Thai Do Ngoc<sup>1</sup>, \*Kien Dang Van<sup>1</sup>, Do Nguyen Thanh<sup>2</sup>

<sup>1</sup>Faculty of Civil Engineering, Hanoi University of Mining and Geology, Hanoi, Vietnam <sup>2</sup>Institute of Mining Science and Technology, Hanoi, Vietnam

\*Corresponding Author, Received: 15 April 2025, Revised: 21 July 2025, Accepted: 26 July 2025

**ABSTRACT:** The increasing need for urbanization has led to the construction of numerous tunnels in urban areas to meet growing transportation demands. A distinctive feature of urban traffic tunnels is the construction of two parallel tunnels located in close proximity to one another. Investigating the mechanical interaction between these twin tunnels during the design phase is crucial. This study employs the finite element method to investigate the mechanical interaction between twin tunnels, extending the study of the deflection angles between the two tunnels at the B-B section of Metro Line No. 1 in Ho Chi Minh City, Vietnam. The key findings are as follows: The normal forces in the lining of the upper tunnel reach their maximum when the offset tunnel configuration has an angular relative position of  $\alpha = 30^{\circ}$ . For piggyback tunnel geometries, increasing depth results in the highest magnitude of normal forces in the lining of the lower tunnel. Due to tunnel interaction, the maximum bending moments in both the upper and lower tunnel linings occur in the offset tunnel configuration with  $\alpha = 45^{\circ}$ . The maximum ground surface settlement caused by twin tunnel construction is greater than that of a single tunnel in greenfield conditions. The side-by-side tunnel configuration results in the smallest ground settlement, while the offset arrangement with  $\alpha = 60^{\circ}$  results in the largest ground settlement. These findings provide valuable insights for the design and construction of twin tunnels in urban environments, emphasizing the importance of understanding tunnel interaction under different configurations.

Keywords: Twin tunnels, Underground construction, Shield tunnelling, Tunnel lining, Settlement

## 1. INTRODUCTION

The development of urban infrastructure often necessitates the construction of tunnels. A defining feature of urban metro systems is the use of two parallel tunnels placed in close proximity. This arrangement introduces significant interactions between the tunnels, leading to increased ground movements and a heightened risk of structural damage.

Several studies have investigated the interaction effects of twin tunnels. Do et al. (2014) reported that these interactions amplify ground movements and increase internal forces in the tunnel linings [1]. Similarly, Wang et al. (2017) demonstrated that the spacing between the centrelines of the tunnels and their diameters significantly influence the internal forces and deformations of the linings [2]. Their findings indicate that the spacing between tunnels has a greater impact on displacement than on stress within the tunnel lining. Furthermore, an increase in the diameter of the second tunnel amplifies the displacement in the lining of the first tunnel.

Do & Wu (2020) investigated twin mountain tunnels and observed that the spacing between tunnels and the angle of rock mass cracks notably affect ground surface settlement patterns and stress distributions around the tunnels [3]. Lin et al. (2024) used a centrifuge-numerical model to study the behavior of twin tunnels, concluding that smaller

tunnel diameters and shallower depths provide higher stability [4]. Similarly, Wang et al. (2024) highlighted that the internal forces and deformations in tunnel linings are highly dependent on the spacing between the tunnels when considering their interaction [5]. Collectively, these studies underscore that factors such as tunnel spacing, diameter, depth, and construction method significantly influence the internal forces and deformation of tunnel linings.

Tunnel boring machines (TBMs) are widely employed for tunnel construction in both hard rock and soft ground conditions. TBMs enhance tunneling efficiency while improving safety for nearby structures. Among the many factors affecting tunneling performance, maintaining appropriate pressure on the tunnel face is crucial for controlling ground settlement, [6-7].

Do et al. (2022) investigated ground surface settlement caused by single and twin tunnel construction in Hanoi, Vietnam [8]. They found that for single tunnel construction, the ground surface settlement curve is symmetrical, consistent with the findings of [9]. However, during twin tunnel construction, the settlement increases, and the settlement curve becomes asymmetrical. This highlights the added complexity and challenges associated with twin tunnel projects.

When constructing tunnels through soft soils in urban areas, maintaining pressure at the tunnel face is critical to stabilizing and balancing the ground around the tunnel. Adequate face pressure reduces subsurface ground movements and minimizes ground settlement above the tunnel [10-14].

Numerous studies have investigated the shape of ground sub-surface movement curves caused by single tunnel construction. Researchers have employed experimental observations, physical modeling, and numerical simulations to predict these movement patterns. It has been widely concluded that the ground settlement curve resulting from single tunnel construction typically follows a Gaussian distribution [15].

To enhance the efficiency of urban traffic tunnel systems, tunnels are often constructed in parallel. However, ground settlement caused by the construction of twin parallel tunnels is generally greater than that caused by a single tunnel [16-19].

There has also been extensive research into the mechanical interactions between twin tunnels and nearby structures. These studies focus on key parameters such as the distance between the tunnels, the proximity of nearby structures, tunnel depth, and tunnel diameter. It has been observed that increasing the distance between the tunnels and nearby structures reduces the magnitude of ground subsurface movements [20-22].

While studies on twin tunnels are growing, much of the earlier research focused on single tunnels, particularly on internal forces. Notable contributions include work by [23-26], these researchers reported that the distribution of internal forces in tunnel linings depend on several factors, including tunnel depth, diameter, cross-sectional shape, and soil type.

Metro lines are commonly constructed with two parallel tunnels, referred to as twin tunnels. However, there is a lack of comprehensive case studies examining the internal force distribution and displacement in the linings of twin tunnels. This highlights the need for further research to explore the relationship between the relative positions of the tunnels and the resulting internal forces and displacements in their linings.

This study employs the finite element method to analyze the mechanical interaction between two tunnels under construction conditions for Metro Line No. 1 in Ho Chi Minh City, Vietnam. The findings provide insights into how the relative positions of the tunnels influence the distribution of internal forces in their linings and ground surface settlement.

The increasing demand for efficient transportation systems in urban areas has led to the construction of an ever-growing number of tunnels. These underground traffic tunnels are frequently designed as twin tunnels, which can be arranged in three primary configurations: side-by-side, offset, or piggyback, as illustrated in Fig. 1.

## 2. RESEARCH SIGNIFICANCE

The construction of two closely spaced parallel tunnels induces mechanical interactions between the tunnels, significantly affecting both the internal forces in the tunnel linings and the extent of ground settlement. This study utilises the finite element method to examine three distinct geometric configurations of twin tunnels: side-by-side, piggyback and offset alignment. By analysing all three scenarios under identical construction and geotechnical conditions, the study provides a clear and quantitative assessment of how tunnel geometry influences structural behavior and ground response. These findings contribute valuable insights for optimizing tunnel design in urban infrastructure projects.

# 3. MATERIAL AND METHODS

This paper employs the finite element method to analyze the mechanical interaction between two parallel tunnels under the construction conditions of Metro Line 1 in Ho Chi Minh City. Ho Chi Minh City, Vietnam's most populous city and its largest cultural and economic hub, is rapidly expanding its infrastructure to meet growing transportation demands, [29, 30].

Metro Line 1 features twin tunnels, including: the Westbound Tunnel (WB Tunnel) and the Eastbound Tunnel (EB Tunnel) constructed using mechanical tunnel boring machines. These tunnels extend from Opera House Station (Km 0+805) to Ba Son Station (Km 1+586), covering a total length of 781 meters each.

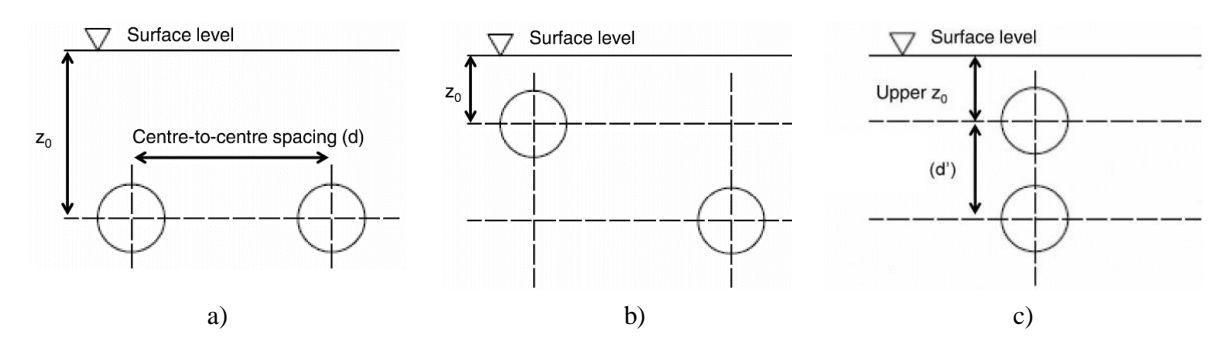


Fig. 1 Geometry of twin tunnels: Twin side-by-side tunnel geometry (a); Twin offset tunnel geometry (b); Twin piggy back tunnel geometry (c)

The tunnel consists of three main sections: The first section, from Km 0+805 to Km 0+930, adopts a piggyback tunnel configuration; The second section, extending from Km 0+930 to Km 1+400, also follows the piggyback twin tunnel layout; The third section, from Km 1+400 to Km 1+586, adopts an offset twin tunnel configuration. At Km 1+586, the alignment transitions to a side-by-side tunnel arrangement with a shared horizontal axis, as illustrated in Figure 2.

The twin tunnels were constructed through various soil layers, including fill, Ac2 (very soft fat clay), As1 (silty fine sand), As2 (medium dense to dense sand), Dilluvium Silt (hard to very hard clay), and Dilluvium Sand (dense to very dense sand). The physical and mechanical properties of these soil layers are summarized in Table 1.

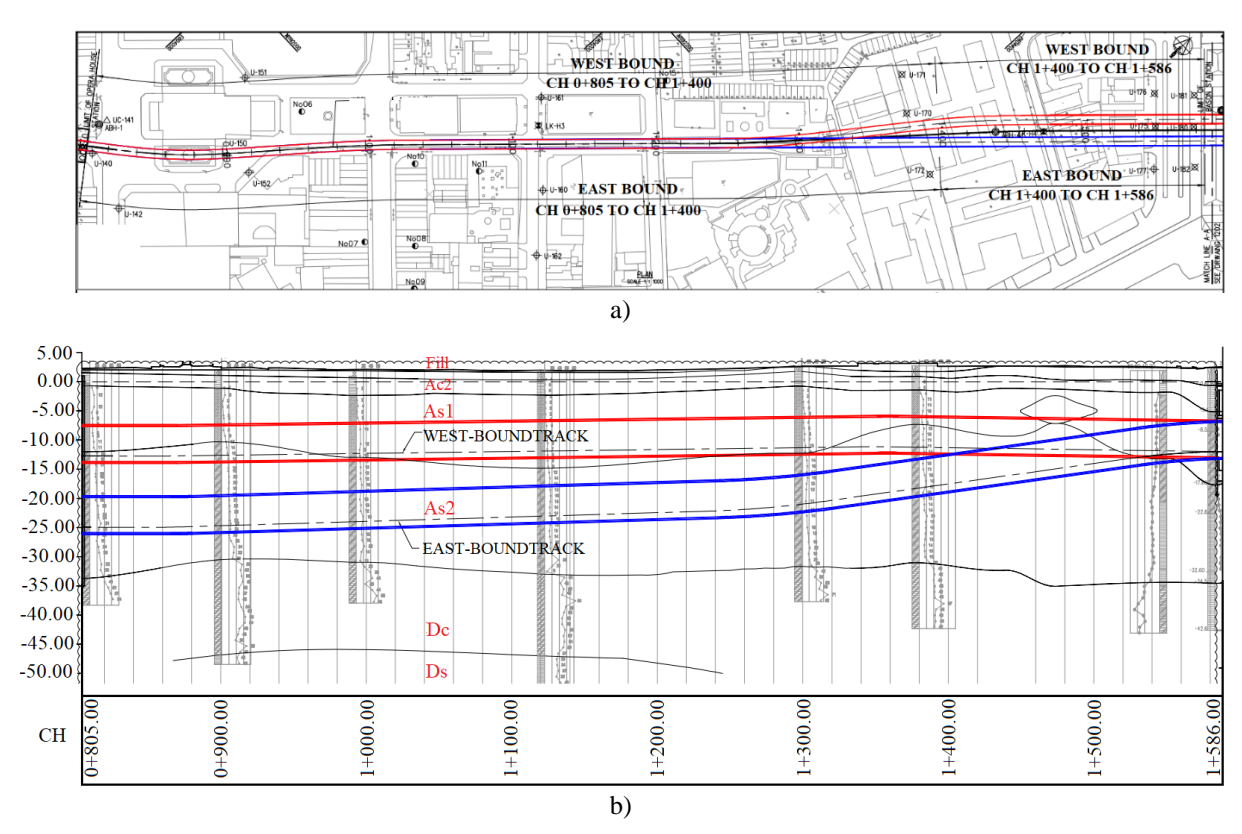


Fig. 2 Plan view of the horizontal alignment (a) and Geotechnical longitudinal section (b) of the metro line 1 in Ho Chi Minh city

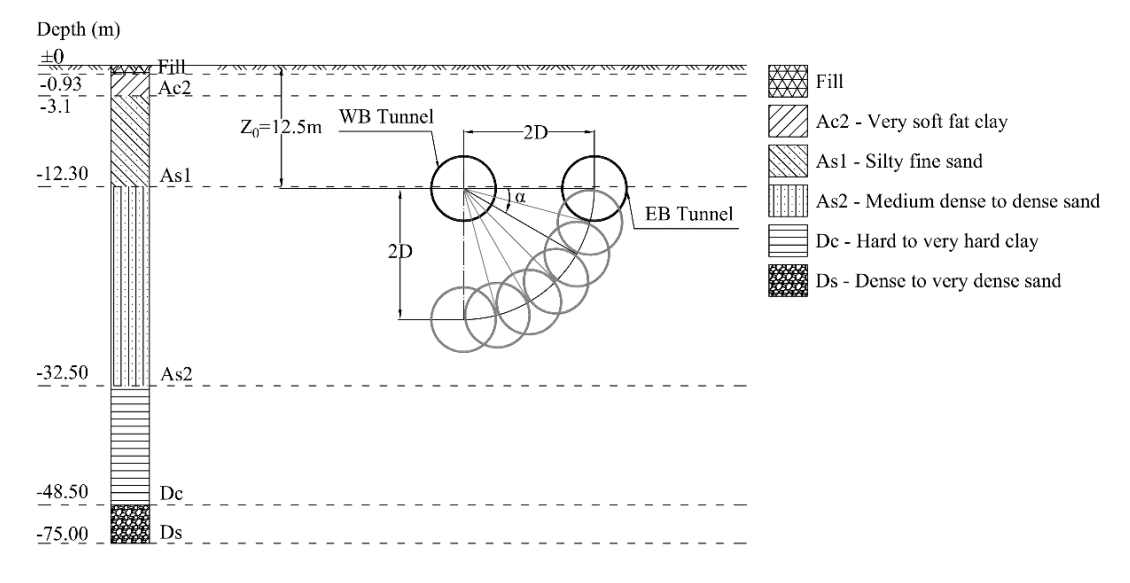


Fig. 3 The soil and twin tunnels geometries used in the finite element analyses

Table 1. Material parameters of the soil layers used in the finite element analyses

Layer	Thick layer l (m)	Unit weight γ (kN/m³)	Young's Modulus E <sub>ref</sub> (kN/m <sup>2</sup> )	ratio	Friction angle φ' (degree)	Dilatancy angle ψ (degree)	Cohesion c <sub>ref</sub> (kN/m <sup>2</sup> )
Fill	0.93	19.0	$\frac{10.0 \times 10^3}{10.0 \times 10^3}$	0.3	25	0	10.0
Ac2-Very soft fat clay	2.17	16.5	$3.0x10^3$	0.3	0	-	10.0
As1-Silty fine sand	9.2	20.5	12.5x10 <sup>3</sup>	0.3	30	0	0.0
As2- Medium dense to dense sand	20.2	20.5	$37.5 \times 10^3$	0.3	33	0	0.0
Dc-Hard to very hard clay	16.0	21.0	$136.0x10^3$	0.3	0	-	170
Ds-Dense to very dense sand	26.5	20.5	$90.0x10^3$	0.3	35	0	0.0

Table 2. Material properties of the tunnel lining

Material	Young's	Axial	Bending	Tunnel	Lining	Unit weigh	Poisson'ratio
properties	Modulus	stiffness	stiffness	diameter	thickness	W	ν
	$E (kN/m^2)$	EA (kN/m)	$EI (kN.m^2/m)$	D (m)	d (m)	(kN/m/m)	
Tunnel lining	$3.5x10^7$	$10.5 \times 10^6$	$7.875 \times 10^4$	6.65	0.3	7.5	0.15

Table 3. Geometry of cases modelled in twin tunnels analyses

Excavation	Angular relative position α (degree)	Tunnel Depth		Horizontal distance between	Vertical distance between	Geometry of twin tunnels	
		WB Tunnel	EB Tunnel	two tunnels	two tunnels	-	
	a (degree)	z (m)	z (m)	x (m)	y (m)		
WB Tunnel.	-	12.5	-	-	-	Single tunnel (Greenfield conditions)	
WB Tunnel,	$\alpha = 0^{\circ}$	12.5	12.5	13.30	0.00	Side-by-side	
EB Tunnel	u – 0	12.3	12.3	13.30	0.00	Side-by-side	
WB Tunnel,	$\alpha = 15^{\circ}$	12.5	15.94	12.85	3.44		
EB Tunnel	u – 13	12.5	13.94	12.63	3.44		
WB Tunnel,	$\alpha = 30^{\circ}$	12.5	19.15	11.52	6.65		
EB Tunnel	u – 30	12.5	19.13	11.32	0.03	_	
WB Tunnel,	$\alpha = 45^{\circ}$	12.5	21.9	9.40	9.40	Offset arrangement	
EB Tunnel	u – 43	12.5	21.9	9.40	9.40	Offset affangement	
WB Tunnel,	$\alpha = 60^{\circ}$	12.5	24.02	6.65	11.52		
EB Tunnel	u – 60	12.3	24.02	0.03	11.32	_	
WB Tunnel,	$\alpha = 75^{\circ}$ 12.5 25		25.35	3.44	12.85		
EB Tunnel	u – 73	12.3	23.33	3.44	12.83		
WB Tunnel,	$\alpha = 90^{\circ}$	12.5	25.80	0.00	13.30	Stacked or piggy back	
EB Tunnel	u – 90	12.3	25.80	0.00	13.30	Stacked of piggy back	

The primary objective of this study is to analyse the interaction mechanisms between twin tunnel linings, considering different geometric configurations of the tunnels. The twin tunnels, each with a diameter of 6.65 m, were constructed with a center-to-center spacing of 2D, where D represents the tunnel diameter. The westbound tunnel was excavated at a depth of  $Z_0 = 12.5$ m (measured to the tunnel axis), while the depth of the eastbound tunnel varied between 12.5 m and 25.8 m. The soil and twin tunnels geometries used in the finite element analyses is depicted in Fig. 3.

Tables 2 and 3 present the material properties of the tunnel linings and the geometric configurations of the twin tunnels at section B-B (Km 0+860) in HCMC \_section B-B used in the finite element analyses.

The numerical model was developed using a plane strain finite element method (FEM) in Plaxis 2D

(Version 20). The soil layers were modelled using the Mohr-Coulomb constitutive law, with the input parameters listed in Table 1. This option allows realistic simulation of the shear strength and volumetric behaviour under tunnel-induced loading. The tunnel lining was represented by linear elastic plate elements, defined in terms of their Young's modulus, Poisson's ratio and thickness, to capture the flexural and axial response of the lining sections, the parameters of which are shown in Table 2. For urban tunnelling using a tunnel boring machine, the volumetric loss used in the model was VL = 0.5%, achieved through the specified shrinkage of the lining elements. The concrete liners, 300 mm thick, were modeled as elastic and isotropic materials. The FEM model boundaries were set at 300 m horizontally and 75 m vertically, comprising 7,092 elements and 58,240 nodes.

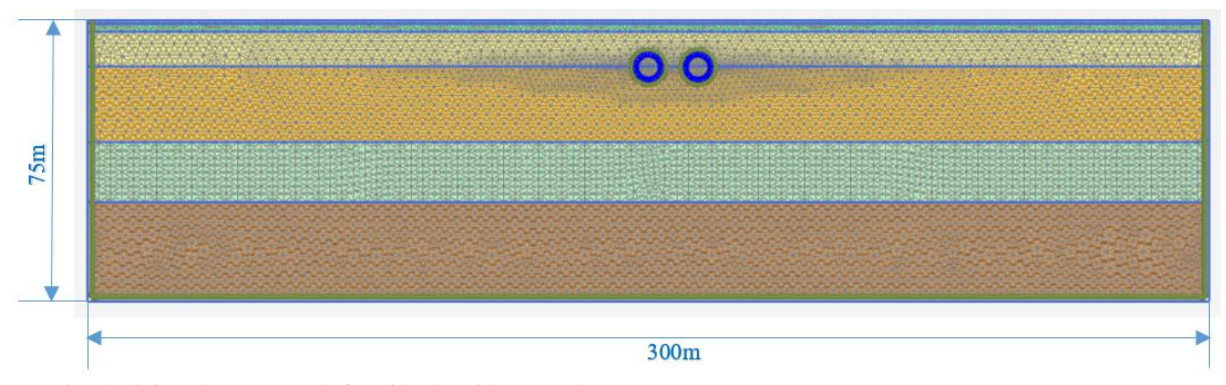


Fig. 4 Finite element mesh for side-by-side tunnels

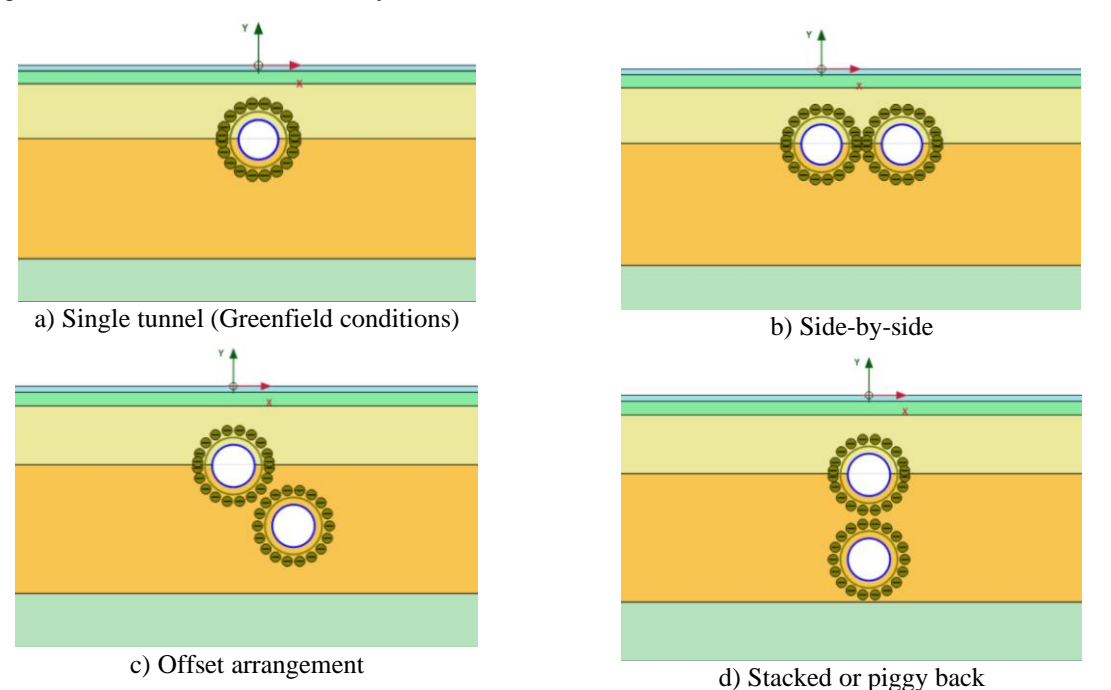


Fig. 5 Simulation diagram for the cases: Single tunnel - Greenfield conditions (a); Side-by-side (b); Offset arrangement (c); Stacked or piggy back (d)

Boundary Conditions, the vertical boundaries were fixed against horizontal displacement but allowed to move vertically, whereas the bottom boundary was fully fixed in both horizontal and vertical directions. In the finite element method using Plaxis, the mesh is automatically generated with a default setting of Medium. However, to accurately capture the mechanical interaction between the two parallel tunnels, the authors reviewed and refined the mesh by subdividing it into smaller elements. In this study, the mesh distribution was set to Fine to improve the precision of the simulation results, as illustrated in Fig. 4.

Metro Line 1 in Ho Chi Minh City, Vietnam, is a shallow tunnel system constructed in soft soil under urban conditions. Under initial conditions, the vertical stresses were assumed to be equal to the unit weight of the soil.

$$\sigma_{v} = \gamma * Z \tag{1}$$

The horizontal stresses are calculated using the appropriate  $K_0$  value:

$$\sigma_h = K_0 * \sigma_v \tag{2}$$

In the Plaxis uses the friction angle value  $\varphi$ ' to calculate the  $K_0$  value (  $K_0 = I - \sin \varphi'$ ).

Plaxis incorporates the concept of volume loss, referred to as the contraction value, to simulate shield-controlled circular tunnels with continuous and uniform linings. Contraction is applied to the structural elements of the tunnel to replicate a reduction in the cross-sectional area. It is defined as the ratio of the reduced cross-sectional area to the original excavated area and is expressed as a percentage.

The numerical model is performed through the following steps:

- Determining the size of the simulation area.
- Assigning initial parameters for the soil layers and tunnel lining.

- Applying boundary conditions.
- Generate the mesh.
- Simulating excavation and lining installation for for WBT and EBT tunnels.
- Ground volume loss was simulated by applying a contraction to the tunnel lining elements for WBT and EBT tunnels.

The research team conducted simulation cases for

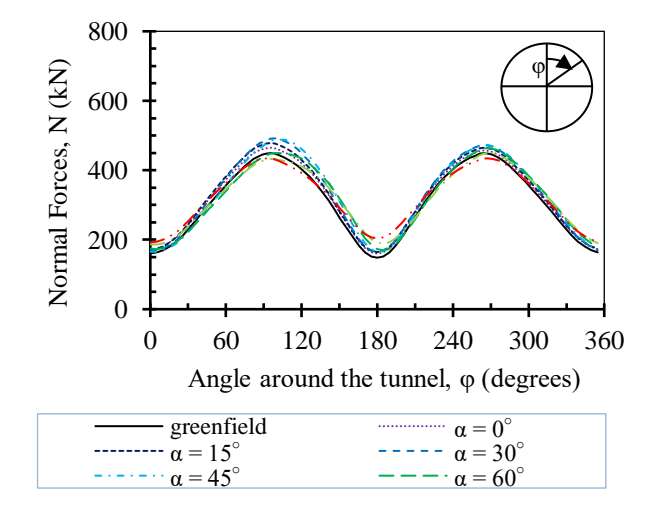
#### 4. RESULTS AND DISCUSSION

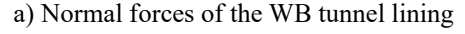
Fig. 6 presents the distribution of normal forces and bending moments around the Westbound (WB) and Eastbound (EB) tunnel linings for various twin tunnel geometries. For the single tunnel case in greenfield conditions (WB tunnel only), the maximum normal force in the WB tunnel lining was 449.23 kN, located above the springlines of the tunnel

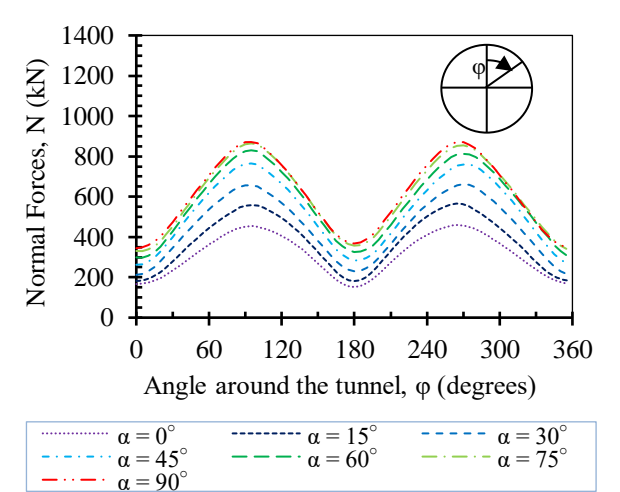
a single tunnel and two parallel tunnels, with relative angles between the tunnels set at  $\alpha=0^\circ, 15^\circ, 30^\circ, 45^\circ, 75^\circ$  and  $90^\circ$ , as summarized in Table 3. Specifically, representative simulation cases for two parallel tunnels, including the side-by-side arrangement ( $\alpha=0^\circ$ ), offset arrangement ( $\alpha=45^\circ$ ), and stacked (or piggyback) arrangement ( $\alpha=90^\circ$ ), are illustrated in Figure 5.

 $(90^{\circ} \div 92^{\circ})$  and  $268^{\circ} \div 270^{\circ}$ . The maximum bending moment was 223.91 kNm, occurring at the invert of the tunnel  $(180^{\circ})$ , consistent with the findings of [25].

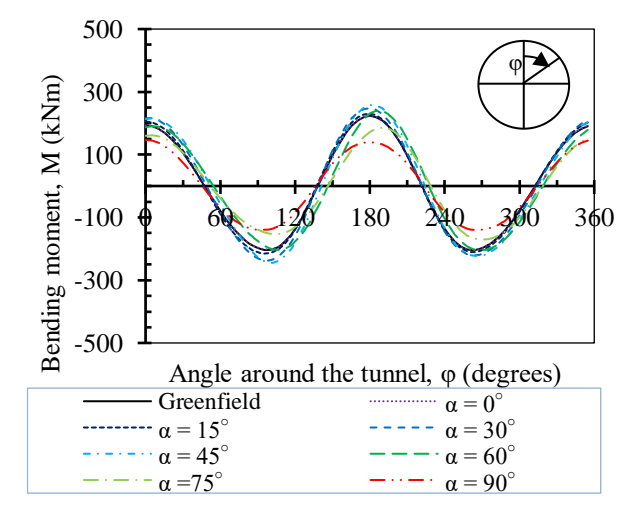
For the side-by-side tunnel configuration ( $\alpha$ =0°): The maximum normal force on the WB tunnel lining increased by 3.49 %, rising from 449.23 kN to 464.92 kN. This force occurred on the right side of the tunnel lining (90°), near the EB tunnel.

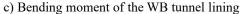


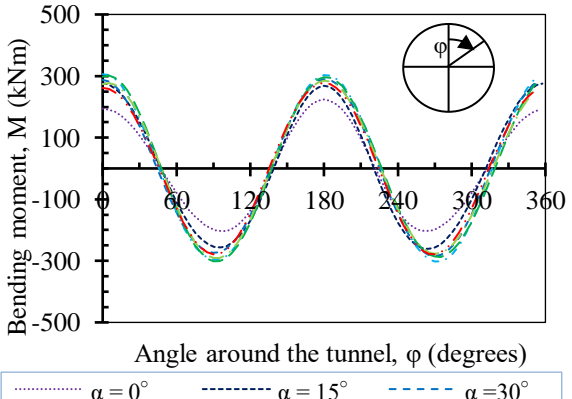




b) Normal forces of the EB tunnel lining







d) Bending moment of the EB tunnel lining

Fig. 6 Distribution of normal forces and bending moments around the WB and EB tunnel lining at different geometry of twin tunnels:  $\alpha = 0^{\circ}$ ,  $15^{\circ}$ ,  $30^{\circ}$ ,  $45^{\circ}$ ,  $60^{\circ}$ ,  $75^{\circ}$ ,  $90^{\circ}$ 

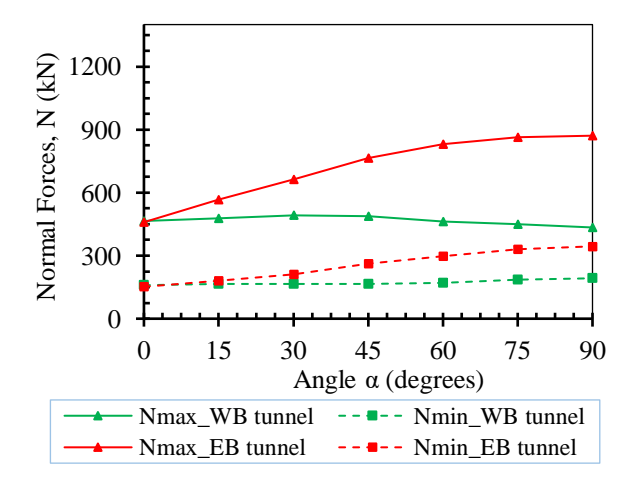
The maximum bending moment on the WB tunnel lining increased slightly by 0.38 %, from 223.91 kNm to 224.75 kNm. For the EB tunnel lining, the maximum normal force was 459.42 kN, occurring on the left side of the tunnel lining (265°), near the WB tunnel. The maximum bending moment was 223.98 kNm, located at the invert of the tunnel (180°).

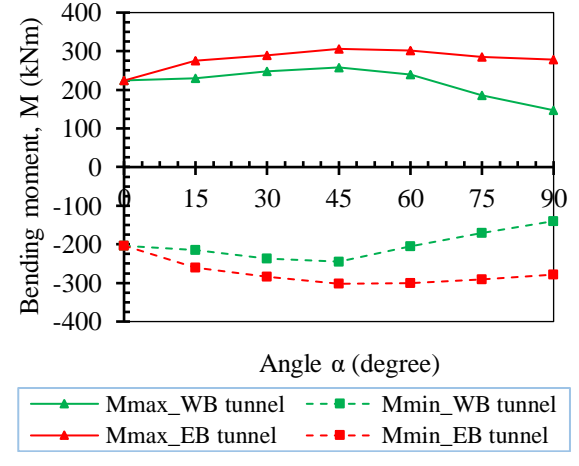
For the offset tunnel configurations  $\alpha=15^{\circ}$ ,  $30^{\circ}$ , 45°, 60°, 75°: The maximum normal forces on the WB tunnel lining increased by 6.48 %, 9.52 %, 8.66 %, 3.24 %, and 0.01 %, respectively, compared to the single tunnel case, with forces rising from 449.23 kN to 478.32 kN, 491.98 kN, 488.15 kN, 463.80 kN, and 449.26 kN. For the EB tunnel lining, the maximum normal forces were 565.99 kN, 662.34 kN, 764.80 kN, 830.02 kN, and 864.22 kN, respectively. The maximum bending moments in the WB tunnel lining for these configurations were 230.47 kNm, 247.85 kNm, 258.02 kNm, 239.08 kNm, and 185.68 kNm, respectively. Correspondingly, the maximum bending moments in the EB tunnel lining were 275.83 kNm, 289.93 kNm, 306.10 kNm, 301.53 kNm, and 284.74 kNm, respectively.

For the piggyback tunnel configuration  $\alpha$ =90°: The maximum normal force in the WB tunnel lining decreased by 3.32 %, from 449.23 kN to 434.31 kN, compared to the single tunnel case. For the EB tunnel lining, the maximum normal force was 871.14 kN. The maximum bending moment in the WB tunnel lining decreased significantly by 34.31 %, from 223.91 kNm to 147.10 kNm. In contrast, the EB tunnel lining experienced a maximum bending moment of 278.41 kNm.

Fig. 7 illustrates the maximum and minimum variations in normal forces and bending moments in the WB and EB tunnel linings for different twin tunnel configurations ( $\alpha = 0^{\circ}$ ;  $15^{\circ}$ ;  $30^{\circ}$ ;  $45^{\circ}$ ;  $60^{\circ}$ ;  $75^{\circ}$ ;  $90^{\circ}$ ). Across all configurations, the EB tunnel lining (upper tunnel) consistently exhibits higher magnitudes of normal forces and bending moments compared to the WB tunnel lining.

The results indicate that the normal forces and bending moments in the tunnel linings are significantly influenced by the geometric configuration of the twin tunnels: The largest normal force in the WB tunnel lining was observed for the offset tunnel configuration at  $\alpha = 30^{\circ}$ , with a magnitude of 491.98 kN. The largest normal force in the EB tunnel lining occurred with the piggyback configuration at  $\alpha = 90^{\circ}$ , reaching 871.14 kN, highlighting the impact of increased depth on the upper tunnel lining. Due to the interaction between the two tunnels, the maximum bending moments were recorded at  $\alpha = 45^{\circ}$  for both the WB and EB tunnel linings, with values of 258.02 kNm and 306.10 kNm, respectively. The results of this study on the normal forces and bending moments in tunnel linings of twin tunnels are consistent with the findings of Koungelis (2007), [27]. For the side-by-side tunnel geometry, the internal forces in both tunnel linings are nearly identical. However, in the piggyback and offset tunnel configurations, the tunnel lining located in the lower position experiences greater internal forces compared to the upper tunnel. This difference highlights the influence of tunnel arrangement on load distribution and structural response.





a) Maximum Normal forces of the WB and EB tunnel lining

b) Maximum Bending moment of the WB and EB tunnel lining

Fig. 7 Effect of the geometry of twin tunnels:  $\alpha = 0^{\circ}$ , 15°, 30°, 45°, 60°, 75°, 90° on the normal forces and bending moment of the WB and EB tunnel lining.

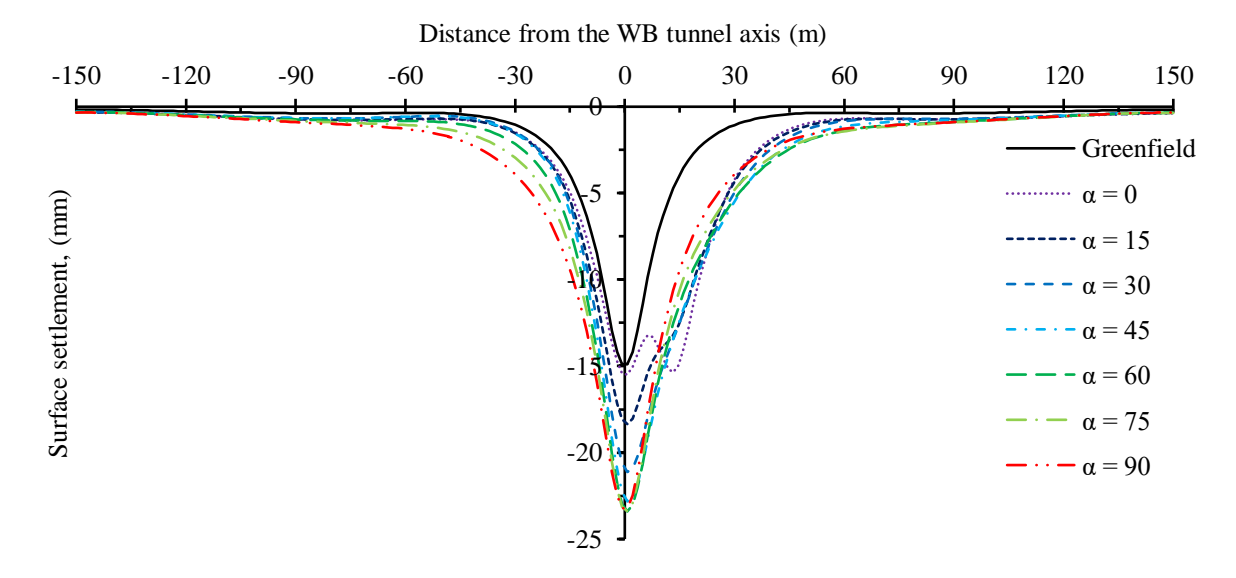


Fig. 8 Effect of the geometry of twin tunnels:  $\alpha = 0^{\circ}$ ,  $15^{\circ}$ ,  $30^{\circ}$ ,  $45^{\circ}$ ,  $60^{\circ}$ ,  $75^{\circ}$ ,  $90^{\circ}$  on the ground surface settlement trough

Fig. 8 shows the ground surface settlement trough caused by the construction of single tunnel and twin tunnels. In case of single tunnel construction, the maximum surface settlement, Smax was 14.88mm and was situated above the centreline of the tunnel, which is in agreement with the reported by Peck (1969). In case of twin tunnels with varying the geometry of twin tunnels:  $\alpha = 0^{\circ}$ , 15°, 30°, 45°, 60°, 75°, 90° the maximum surface settlement, Smax were 15.49mm, 18.35mm, 21.12mm, 22.83mm, 23.40mm, 23.39mm, 23.21mm respectively.

These results show that when constructing twin tunnels causes a larger value of ground settlement than constructing single tunnel in the greenfield conditions. Among twin tunnel configurations, the minimum surface settlement value, Smin of 15.49mm was observed for side-by-side tunnels ( $\alpha = 0^{\circ}$ ), while the maximum surface settlement value, Smax of 23.40mm was observed for the offset arrangement with  $\alpha = 60^{\circ}$ . The results of this study on ground settlement induced by two parallel tunnels are consistent with the findings of Hunt (2005) [28]. Specifically, the settlement trough caused by twin tunnels is greater than that of a single tunnel. In the case of side-by-side tunnel geometry, the width of the settlement trough is wider. However, for piggy back and offset tunnel configurations, the maximum settlement is more pronounced.

We acknowledge that the use of 2D numerical modeling software presents certain limitations when compared to fully three-dimensional (3D) analyses. Specifically, 2D models may not fully capture the spatial variability of ground response, face-pressure effects, or complex interactions along the tunnel axis.

Additionally, simplifications such as the assumption of constant lining stiffness and the omission of groundwater influence may reduce the accuracy of results in certain contexts. Future research could address these limitations through three-dimensional modeling, parametric studies of face-pressure variations, and comparisons with field-monitoring data to enhance model validation and reliability.

## 5. CONCLUSION

The construction of urban tunnels offers a sustainable solution for meeting traffic demands and fostering economic development. To optimize urban traffic flow, tunnels are often designed as twin tunnels. The mechanical interaction between these tunnels impacts the internal forces within the tunnel lining. Consequently, the geometry of the two tunnels significantly influences their stability. This study investigates the effect of twin tunnels geometry on the distribution of internal forces in the tunnel linings and ground surface settlement. Based on this research, the following conclusions can be drawn:

- For twin tunnel constructions, the interaction between the tunnels results in greater normal forces and bending moments in the tunnel linings compared to single tunnel constructions in greenfield conditions.
- In the three types of twin tunnels geometry: sideby-side tunnels, offset tunnels, piggyback tunnels, the value of normal forces in the lower tunnel lining is largest in the piggyback tunnels. The normal forces in the upper tunnel lining is largest in the offset tunnels when  $\alpha=30^\circ$ .
- In the twin offset tunnel configuration with  $\alpha = 45^{\circ}$ , the bending moments in both the upper and lower

tunnel linings are largest.

- The maximum ground surface settlement value caused by the construction of twin tunnels is larger than that found for single tunnel in the greenfield conditions, the geometry of the side by side tunnels with  $\alpha=0^{\circ}$  causes the smallest ground settlement value, while the offset arrangement with  $\alpha=60^{\circ} \div 75^{\circ}$  causes the largest ground settlement value.

This study investigated the internal lining forces and ground settlements associated with three twin tunnel geometry: side-by-side, piggyback, and offset, using the finite element method in Plaxis. The results demonstrate that tunnel geometry has a significant impact on both the magnitude of internal lining forces and the ground settlement profile. Among the configurations analysed, side-by-side the arrangement resulted in more balanced lining forces and reduced surface settlement. These findings underscore the importance of selecting an appropriate tunnel geometry, particularly favoring the side-byside geometry, to optimize structural performance and minimize ground disturbance in twin tunnel design.

#### 6. ACKNOWLEDGMENTS

This research was funded by Hanoi University of Mining and Geology under grant number T25-41. This funding is greatly appreciated.

## 7. REFERENCES

- [1] Do N.A., Dias D., Oreste P., Maigre I.D., Three-dimensional numerical simulation of a mechanized twin tunnels in soft ground. Tunnelling and Underground Space Technology, 42, 2014, pp. 40-51. https://doi.org/10.1016/j.tust.2014.02.001
- [2] Wang H.N., Zeng G.S, Utili S., Jiang M.J, Wu L., Analytical solutions of stresses and displacements for deeply buried twin tunnels in viscoelastic rock. International Journal of Rock Mechanics & Mining Sciences, 93, 2017, pp. 13-29. https://doi.org/10.1016/j.ijrmms.2017.01.002
- [3] Do T.N., Wu J.H., Verifying discontinuous deformation analysis simulations of the jointed rock mass behavior of shallow twin mountain tunnels. International Journal of Rock Mechanics and Mining Sciences, 130, 2020, pp. 104322. https://doi.org/10.1016/j.ijrmms.2020.104322
- [4] Lin W.S.E., Yang Z., Ni P., Chen Y., Damage analysis of buried pipelines subjected to side-by-side twin tunneling based on centrifuge and numerical modeling. Tunnelling and Underground Space Technology, 146, 2024, pp. 105647.
  - https://doi.org/10.1016/j.tust.2024.105647

- [5] Wang C., Li X., Song D., Wang E., He Z., Tan R., Structural response of former tunnel in the construction of closely-spaced cross-river twin tunnels. Tunnelling and Underground Space Technology, 147, 2024, pp. 105652. https://doi.org/10.1016/j.tust.2024.105652
- [6] Jonak J., Kuric I., Droździel P., Gajewski J., Saga M., Prediction of load on the cutting tools in tunnel boring machines. Acta Montanistica Slovaca, 25(4), 2020, pp. 444-452. https://doi.org/10.46544/AMS.v25i4.01
- [7] Mahmoodzadeh A., Ali H.F.H., Ibrahim H.H., Mohammed A.H., Rashidi S., Mahmood L., Ali M.S., Application of Autoregressive Model in the Construction Management of Tunnels. Acta Montanistica Slovaca, 27(3), 2022, pp. 581-588. https://doi.org/10.46544/AMS.v27i3.02
- [8] Do N.T., Protosenya A.G. and Vo C.C.T., Prediction of ground surface settlement induced by twin tunnelling in urban areas. Journal of Mining and Earth Sciences, 63(3a), 2022, pp. 22-28.
  - https://doi.org/10.46326/JMES.2022.63(3a).03
- [9] Peck R.B., Deep excavations and tunnelling in soft ground. In: Proc. 7th ICSMFE, State-of-theart, Mexico City, 1969, pp. 225-290.
- [10] Protosenya A.G., Belyakov N.A., Do N.T., The development of prediction method of earth-pressure balance and earth surface settlement during tunneling with mechanized tunnel boring machines. Journal of Mining Institute, 211, 2015, pp. 53-63.
- [11] Protosenya A.G., Alekseev A.V., Verbilo P.E., Prediction of the stress-strain state and stability of the front of tunnel face at the intersection of disturbed zones of the soil mass, Journal of Mining Institute, 254, 2022, pp. 252-260. https://doi.org/10.31897/PMI.2022.26
- [12] Nematollahi M., Dias D., Twin earth pressure balance tunnelling monitoring and numerical study of an urban case. Geotechnical Engineering, 176(6), 2023, pp. 662–674. https://doi.org/10.1680/jgeen.21.00165
- [13] Ma S., Li J., Li Z., Critical support pressure of shield tunnel face in soft-hard mixed strata. Transportation Geotechnics, 37, 2022, pp. 100853. https://doi.org/10.1016/j.trgeo.2022.100853
- [14] Khan Z.A., Sadique M.R., Samanta M., Evaluation of Surface Settlement Due to Construction of Twin Transportation Tunnels in Soils. Transportation Infrastructure Geotechnology, 11, 2024, pp. 934-955. https://doi.org/10.1007/s40515-023-00308-z
- [15] Addenbrooke T.I., Potts D.M., Twin tunnel interaction: surface and subsurface effects. International Journal of Geomechanics, 1(2), 2001, pp. 249-271.
- [16] Chee-Min K., Thanath G., Nurfatin Afifah A. R., Hisham M., Volume loss caused by tunnelling in

- kenny hill formation. International Journal of GEOMATE, 16(54), 2019, pp.164 169. https://doi.org/10.21660/2019.54.8316
- [17] Jiaxin L., Xiaowu T., Tianqi W., Weikang L., Keyi L., Qingqing X., Development of surface settlement of twin tunnels under the influence of the river. International Journal of GEOMATE, 26(116), 2024, pp. 126-133. https://doi.org/10.21660/2024.116.g13159
- [18] Islam M.S., Iskander M., Twin tunnelling induced ground settlements: A review. Tunnelling and Underground Space Technology, 110, 2021, pp. 103614. https://doi.org/10.1016/j.tust.2020.103614
- [19] Islam M.S., Iskander M., Ground settlement caused by perpendicularly crossing twin tunnels, a parametric study. Tunnelling and Underground Space Technology, 146, 2024, pp. 105657. https://doi.org/10.1016/j.tust.2024.105657
- [20] Zhu C.W., Wu W., Ying H.W., Gong X.N., Guo P.P., Drainage-induced ground response in a twintunnel system through analytical prediction over the seepage field. Underground Space, 7(3), 2022, pp. 408-418. https://doi.org/10.1016/j.undsp.2021.09.004
- [21] Zheng G., Wang R., Lei H., Zhang T., Guo J., Zhou Z., Relating twin-tunnelling-induced settlement to changes in the stiffness of soil. Acta Geotech, 18, 2023, pp. 469–482. https://doi.org/10.1007/s11440-022-01541-5
- [22] Khoo C.M., Hisham M., Phromphat T., Some insights into three-dimensional modeling of Tunnel excavation. International Journal of GEOMATE, 27(120), 2024, pp. 27-39. https://doi.org/10.21660/2024.120.4393
- [23] Pabodha K. K., Kannangara M., Ding Z., Zhou W., Surface settlements induced by twin tunneling in silty sand. Underground Space, 7(1), 2022, pp. 58-75. https://doi.org/10.1016/j.undsp.2021.05.002
- [24] Do N.A., Dias D., Oreste P., Maigre I.D., 2D numerical investigation of segmental tunnel lining

- behavior. Tunnelling and Underground Space Technology, 37, 2013, pp. 115-127. https://doi.org/10.1016/j.tust.2013.03.008
- [25] Marwan A., Gall V.E., Alsahly A., Meschke G., Structural forces in segmental linings: processoriented tunnel advance simulations vs. conventional structural analysis. Tunnelling and Underground Space Technology, 111, 2021, pp. 103836.
  - https://doi.org/10.1016/j.tust.2021.103836
- [26] Do N.A., Dias A., Golpasand M.B., Dang V.K., Nait-Rabah, Q., Pham, V.V., Dang, T.T., Numerical analyses of twin stacked mechanized tunnels in soft grounds – Influence of their position and construction procedure, Tunnelling and Underground Space Technology, 130, 2022, pp. 04734.
  - https://doi.org/10.1016/j.tust.2022.104734
- [27] Koungelis D., Tools for numerical modelling of tunnelling interactions. Doctor of philosophy, Durham University, England, 2007, pp. 1-307.
- [28] Hunt D.V. L., Predicting the ground movements above twin tunnels constructed in London Clay. Doctor of philosophy, University of Birmingham. Birmingham, England, 2005, pp. 1-355.
- [29] HCMC-CP., Ho Chi Minh city Urban railway construction project: Ben Thanh Suoi Tien section (Line1). Bored tunnel segmental lining-technical design report, Underground section Km 0+615 to Km 2+360. HCMC Urban Railway Management Board, Ho Chi Minh city, Vietnam, 2016, pp. 1-694.
- [30] HCMC-CP., Ho Chi Minh city Urban railway construction project: Ben Thanh Suoi Tien section (Line1). Bored tunnel segmental lining-technical design report (Third submission), HCMC Urban Railway Management Board, Ho Chi Minh city, Vietnam, 2016, pp. 1-141.

Copyright <sup>©</sup> Int. J. of GEOMATE All rights reserved, including making copies, unless permission is obtained from the copyright proprietors.